

Global Millimeter-Wave Observations of Precipitation Using AMSU on the NOAA-15 Satellite

F. W. Chen and D. H. Staelin
Massachusetts Institute of Technology
77 Massachusetts Avenue, Room 26-341
Cambridge, MA 02139-4307

Abstract - This paper extends prior work on estimating instantaneous rain rates using data from the NASA Advanced Microwave Sounding Unit (AMSU) aboard the NOAA-15 satellite (Staelin and Chen, IEEE TGARS, vol. 38, pp. 2322-32, 2000) by utilizing more AMSU channels, training orbits, and seasons of the year, and by 1) inferring 15-km perturbations for the 50-km resolution channels, 2) adapting the algorithm to include cold dry atmospheres, 3) training using only the most reliable NOAA NEXRAD 3-GHz radar data, 4) applying the method to snowfall rate retrievals, and 5) preliminary global testing of the resulting algorithm over land and sea. The 15- and 50-km resolution algorithms were tested at AMSU rain rates up to 160 and 100 mm/h, respectively.

I. INTRODUCTION

AMSU-A views 30 spots cross-track with ~50-km resolution near nadir at 15 frequencies from 23.6 to 91 GHz. AMSU-B views 90 spots with ~15-km resolution at 5 frequencies from 87 to 192 GHz. The prior work utilized the scan angle, the spatial cold-spot perturbations in AMSU-A channels 4-6 (52-55 GHz), and the radiances near 183 ± 7 and 183 ± 1 GHz, all at ~50-km spatial resolution. The current work additionally incorporates spatial cold-spot perturbations in AMSU-A channels 7 and 8 (54-56 GHz), the radiance near 183 ± 3 GHz, temperature-profile information obtained from AMSU-A channels 4-8 (52-56 GHz), and humidity-profile information obtained from the following channels: AMSU-A window channels 1, 2, 3, and 15, and AMSU-B radiances near 150, 183 ± 1 , 183 ± 3 , and 183 ± 7 GHz. Use of the AMSU-B 150-GHz and 183 ± 3 -GHz channels is now possible due to a significant reduction in radio-frequency interference. These additions provide more information concerning atmospheric temperature and humidity profiles, which can improve precipitation-rate retrievals. For example, warm humid atmospheres can more readily support intense precipitation. Retrieval improvements were also obtained in polar regions by using the 183 ± 3 -GHz channel for the first time to flag potentially precipitating regions when the troposphere is so cold and dry that the 183 ± 7 -GHz channel normally used for this purpose sees the surface and becomes unreliable.

The prior AMSU/NEXRAD comparisons were confined to two frontal passages and two hurricane passes. These were generally characterized by large precipitating cells that were resolved at 50-km resolution, whereas the current data include many small intense convective cells that were not resolved by AMSU-A. The contributions of these extremely intense small cells to regional precipitation rates are therefore underestimated by standard 50-km resolution AMSU retrievals; these underestimates have been reduced by utilizing the 15-km resolution of AMSU-B to detect and characterize these small intense cells. Also, current AMSU/NEXRAD comparisons involve data from 38 orbits distributed over one calendar year and involve a much more representative sample of precipitation types than before.

In addition to the increased number of variables used to estimate rain rate, another improvement has been the use of only the most reliable NEXRAD data for which multiple NEXRAD beams sense the rain. Previously, data from any point in the eastern U.S. could have been used to train and test the algorithm. Now, only data obtained beyond 30 km but within 110 km of each site were utilized for training.

These studies also revealed cases where snowfall was evident in AMSU data and also on the ground. These retrieved precipitation images exhibit no evident discontinuities across the rain-snow boundaries. This sensitivity to snowfall and insensitivity to rain-snow boundaries follows from the same cell-top physics responsible for AMSU's sensitivity to rain rate. The convective cell tops sensed by AMSU generally lie above those zones where precipitation might or might not melt before impact, and are not greatly affected either way. This all-season training, largely surface-blind, has enabled plausible precipitation retrievals to be obtained globally with the same algorithm over land and sea, and from the tropics to latitudes up to $\pm 72^\circ$.

II. PERTURBATIONS AT 15-KM RESOLUTION

The following presents our first retrievals at 15-km resolution that utilize the 54-GHz data essential at high rain rates. Our previous estimator [1] operated on data at 50-km resolution to retrieve rain rate at 50-km resolution, which can leave small intense precipitation cells undetected. In order to sense such small cells, rain-rate retrievals at 15-km

This work was supported by the National Aeronautics and Space Administration under grant NAG5-7487 and contract NAS5-31376.

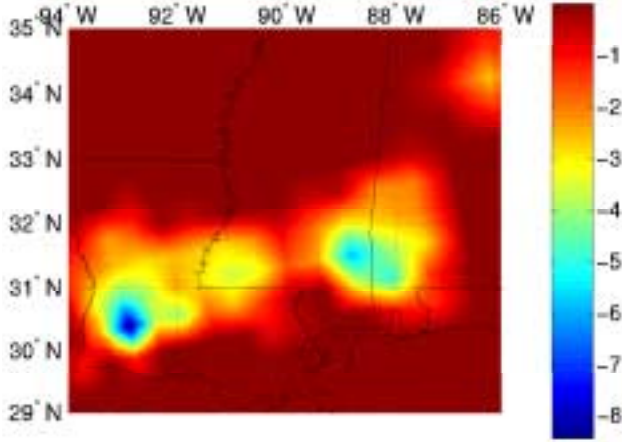


Fig. 1. 52.8-GHz perturbations (K) at 50-km resolution

resolution are desirable, and all perturbation inputs to the estimator should have 15-km resolution. By itself, interpolation of the 50-km 54-GHz perturbation images to each AMSU-B pixel would not suffice. First, cloud-induced perturbations are calculated at 183 ± 7 GHz because this frequency appears to be the most reliable for detecting potentially precipitating pixels. When the atmosphere is so cold and dry that 183 ± 7 GHz becomes unreliable for this purpose, the 183 ± 3 -GHz channel is substituted. The 53.6-GHz temperature sounding channel is used to decide when the 183 ± 3 -GHz channel should be used. The resulting 183-GHz perturbation image $\Delta T_{15,183}$ is then filtered to 50-km to yield $\Delta T_{50,183}$. Then, for each of channels 4-8, the 15-km, 54-GHz perturbations are estimated using the following formula:

$$\Delta T_{15,54} = (\Delta T_{15,183} / \Delta T_{50,183}) \Delta T_{50,54} \quad (1)$$

Fig. 1 shows 52.8-GHz perturbations observed on Sept. 13, 2000, from 0116 to 0119 UTC at 50-km resolution, and Fig. 2 shows the perturbations inferred at 15-km resolution

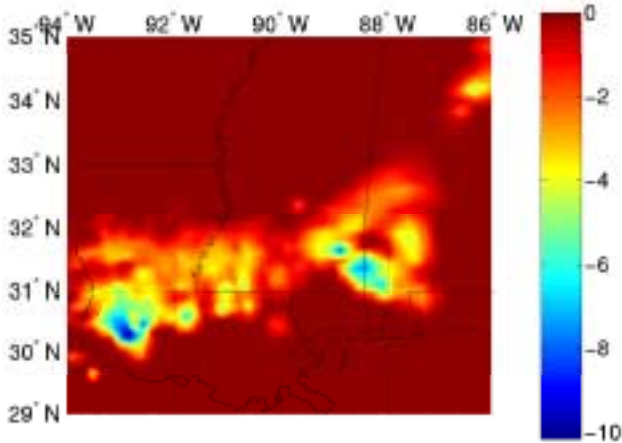


Fig. 2. 52.8-GHz perturbations (K) at 15-km resolution

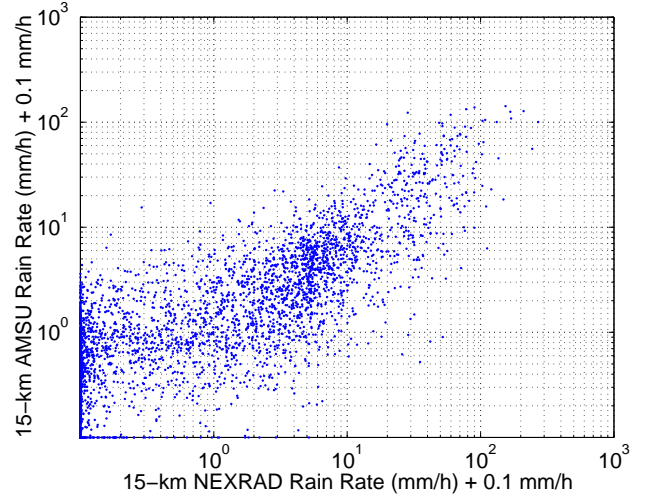


Fig. 3. Comparison of AMSU and NEXRAD estimates of rain rate at 15-km resolution

using the same data.

III. PRECIPITATION-RATE RETRIEVALS

Only scan angles less than 43° from nadir were analyzed; thus 6 of the 90 AMSU-B scan angles were omitted. Fig. 3 is a scatter plot relating nearly simultaneous AMSU and NEXRAD precipitation estimates for 15-km spots, where the 2-km NEXRAD radar precipitation estimates have been convolved with the AMSU 15-km antenna pattern and then subsampled at the center of each AMSU beam. Time offsets between AMSU and NEXRAD are generally less than ~ 7 minutes. Approximately 7580 15-km precipitating samples were used for training, 3790 for testing, and 3790 for validation. All three categories provided consistent results.

The pixels in the testing set were partitioned into eight

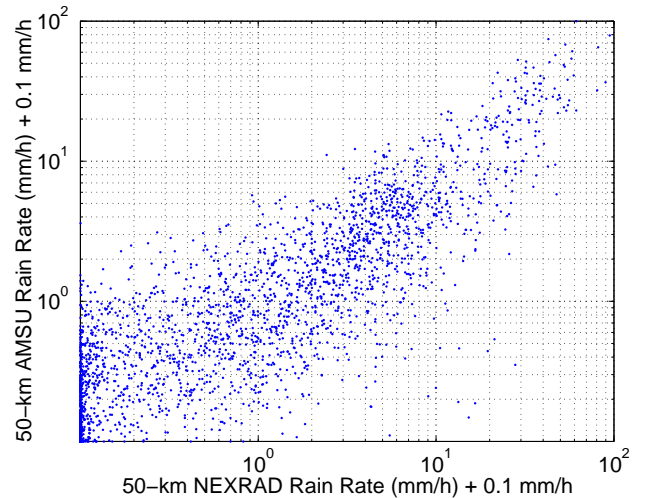


Fig. 4. Comparison of AMSU and NEXRAD estimates of rain rate at 50-km resolution

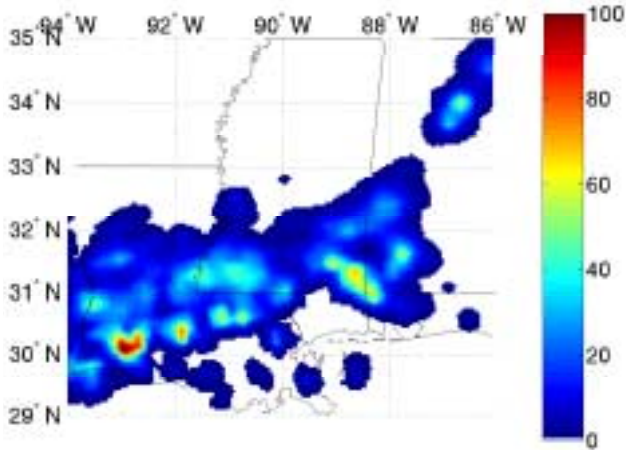


Fig. 5. NEXRAD 15-km precipitation-rate retrievals (mm/h)

NEXRAD rain -rate categories: <0.5, 0.5-1, 1-2, 2-4, 4-8, 8-16, 16-32, and >32 mm/h. For the set of 38 orbits, the rms discrepancies between these 15-km resolution AMSU and NEXRAD retrievals for each category are 1.0, 2.0, 2.3, 2.7, 3.5, 6.9, 19.0, and 42.9 mm/h, respectively. The 50-km AMSU retrievals are obtained by smoothing the 15-km AMSU retrievals to 50-km resolution. Fig. 4 is a scatter plot relating AMSU and NEXRAD precipitation rate at 50-km resolution for the same orbits. The rms discrepancies for the same categories are 0.5, 0.9, 1.1, 1.8, 3.2, 6.6, 12.9, and 22.1 mm/h, respectively. Both scatter plots show promising agreement.

Figs. 5 and 6 show the precipitation-rate retrievals of NEXRAD and AMSU, respectively, over the same set of precipitation cells described in Figs. 1 and 2.

The retrieval algorithm was also applied to data outside the U.S. and, when compared to 183±7-GHz data and climatological norms, was found to give plausible retrievals.

This study furthermore provided an opportunity for

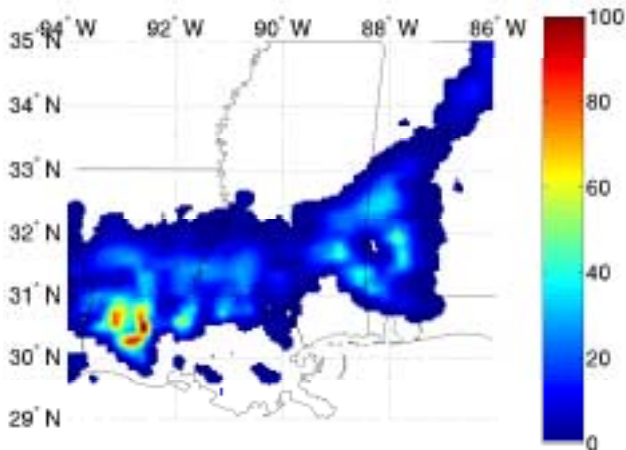


Fig. 6. AMSU 15-km precipitation-rate retrievals (mm/h)

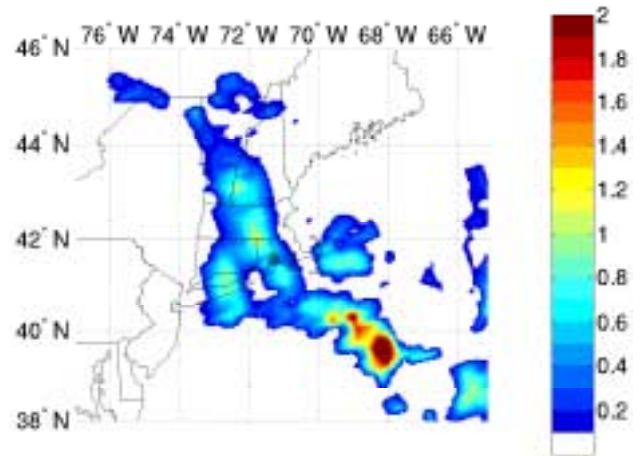


Fig. 7. AMSU precipitation-rate retrievals (mm/h) over a snowstorm

evaluation of radar data. The rms discrepancies between AMSU and NEXRAD retrievals were separately calculated over all points more than 110 km from any radar. For NEXRAD precipitation rates below 16 mm/h, the rms discrepancies were approximately 40% greater than those computed for test points close to the radars, confirming that NEXRAD rain rates tend to be less accurate more than 110 km from each radar site. Most points in the eastern U.S. are in this more distant category. At rain rates greater than 16 mm/h, the accuracies beyond 110 km were more comparable.

IV. SNOWFALL

The present retrieval algorithm was applied to data taken over a major New England snowstorm on 5 March 2001. Fig. 7 shows the resulting precipitation rate image. Precipitation rates up to 1.5 mm/h were retrieved.

ACKNOWLEDGMENT

The authors wish to thank P.W. Rosenkranz, E. Williams, and M.M. Wolfson for helpful discussions, and S.P.L. Maloney, C. Lebell, and the Weather Services International Corporation, Boston, MA, for assistance with the NEXRAD data.

REFERENCES

- [1] D. H. Staelin and F. W. Chen, "Precipitation observations near 54 and 183 GHz using the NOAA-15 satellite", *IEEE Trans. Geosci. and Remote Sensing*, vol. 38, no. 5, Sept. 2000, pp. 2322-2332.